

# Enhancement of coherent X-ray diffraction from nanocrystals by introduction of X-ray optics

**Ian K. Robinson**

*Department of Physics, University of Illinois, Urbana, IL 61801, USA.*

**Franz Pfeiffer**

*Swiss Light Source, Paul Scherrer Institut, CH-5232 Villigen PSI, Switzerland.  
and Department of Physics, University of Illinois, Urbana, IL 61801, USA.*

**Ivan A. Vartanyants**

*Department of Physics, University of Illinois, Urbana, IL 61801, USA.*

**Yugang Sun and Younan Xia**

*Department of Chemistry, University of Washington, Seattle, WA 98195, USA.*

[ikr@uiuc.edu](mailto:ikr@uiuc.edu)

**Abstract:** Coherent X-ray Diffraction is applied to investigate the structure of individual nanocrystalline silver particles in the 100nm size range. In order to enhance the available signal, Kirkpatrick-Baez focusing optics have been introduced in the 34-ID-C beamline at APS. Concerns about the preservation of coherence under these circumstances are addressed through experiment and by calculations.

© 2003 Optical Society of America

**OCIS codes:** (030.1670) Coherent optical effects; (030.6140) Speckle.

---

## References and links

1. D. Sayre, "Imaging Processes and Coherence in Physics," Springer Lecture Notes in Physics **112**, 229 (1980).
2. J. Miao, P. Charalambous, J. Kirz and D. Sayre, "Extending the methodology of X-ray crystallography to allow imaging of micrometer-sized non-crystalline specimens," Nature **400**, 342 (1999).
3. G. J. Williams, M. A. Pfeifer, I. A. Vartanyants and I. K. Robinson, "Three-dimensional Imaging of Microstructure in Gold Nanocrystals," Phys. Rev. Lett. **90**, 17 (2003).
4. J. Miao, T. Ishikawa, B. Johnson, E. H. Anderson, B. Lai and K. O. Hodgson, "High Resolution 3D X-Ray Diffraction Microscopy," Phys. Rev. Lett. **89** (2002).
5. I. K. Robinson, I. A. Vartanyants, G. J. Williams, M. A. Pfeifer and J. A. Pitney, "Reconstruction of the Shapes of Gold Nanocrystals using Coherent X-ray Diffraction," Phys. Rev. Lett. **87**, 19 (2001).
6. I. K. Robinson, C. A. Kenney-Benson and I. A. Vartanyants, "Sources of Decoherence in Beamline Optics," Physica B **336** 56-62 (2003)
7. M. R. Howells, D. Cambie, R. M. Duarte, S. Irick, A. A. MacDowell, H. A. Padmore, T. R. Renner, S. Rah, and R. Sandler, "Theory and practice of elliptically bent x-ray mirrors," Opt. Eng. **39** 2748-2762 (2000)
8. Yugang Sun and Younan Xia, "Shape-Controlled Synthesis of Gold and Silver Nanoparticles," Science **298**, 2176 (2002).
9. T. Kupp, B. Blank, A. Deyhim, P. H. Fuoss, C. A. Benson and I. K. Robinson, "Development of a Double Crystal Monochromator," Proceedings of SRI conference, Berkeley (2003).
10. J. L. Libbert, J. A. Pitney and I. K. Robinson, "Asymmetric Fraunhofer Diffraction from Roller Blade Slits," J. Synchrotron Radiation **4** 125-127 (1997).
11. K. A. Nugent, T. E. Gureyev, D. F. Cookson, D. Paganin, and Z. Barnea, "Quantitative Phase Imaging Using Hard X Rays," Phys. Rev. Lett. **77** 2961-2964 (1996)
12. T. E. Gureyev, "Composite Techniques for Phase Retrieval in the Fresnel Region," Opt. Commun. **220** 49-58 (2003).
13. K. A. Nugent, Melbourne University, private communication.

## 1. Introduction

Nanocrystals are potentially important materials because their physical and chemical properties can deviate significantly from the bulk crystalline phase. It is generally found that the "nanophase" length scale, where these effects become strong, starts at 100nm, extending downwards. Once these deviations are understood, they can be tailored for the purposes of engineering new industrial materials. New technologies are emerging for the fabrication of the materials. Structural characterization of nanomaterials is usually achieved by electron microscopy, even though there are serious limitations of multiple scattering and penetration depth. X-rays are less interacting than electrons, so potentially can avoid the problems, but have a serious drawback of not allowing direct imaging because of the lack of suitable lenses. This has led to the development of Fourier inversion methods based on iterative computations, which are starting to have success [1-3].

Our goal is to analyse the internal structure of nanocrystals by inversion of the coherent X-ray diffraction (CXD) patterns surrounding their Bragg peaks. A Charge-Coupled Device (CCD) X-ray detector is placed sufficiently far away from the sample to fully resolve the fringes that arise from the limited spatial extent of the nanocrystal. The diffraction pattern must be *oversampled* with respect to the spatial Nyquist frequency for the subsequent inversion to work, which means the number of pixels per fringe must be greater than two, preferably much greater [1,2]. Three dimensional (3D) data are then readily obtained by making small angular deviations of the sample orientation around the Bragg condition [3]. The 3D data naturally lie on a Cartesian grid suitable for inversion using Fast Fourier Transform (FFT) methods. The advantage of using Bragg diffraction [3], rather than forward scattering [4], is that the angular range containing a 3D data set is  $0.5^\circ$ , rather than  $180^\circ$

Coherence of the illumination is a necessary condition for these experiments to work. Coherence is needed so that scattering from all parts of the nanocrystal sample can interfere at the detector to create fringes. Lateral coherence lengths must exceed the lateral spatial dimension of the crystal; longitudinal coherence must exceed the maximum optical path-length difference (OPLD) through the sample, which can be quite large under a Bragg diffraction condition. In practice, using 3rd generation sources of synchrotron radiation (SR), the inherent lateral coherence lengths are in the range 5–100 $\mu\text{m}$ , considerably greater than the 100nm sample size of interest. The longitudinal coherence length is inversely related to the bandwidth of the radiation, which is commonly determined by Si crystal diffraction. This is typically a bit smaller than 1 $\mu\text{m}$ , so usually sufficient to satisfy the OPLD in crystals smaller than 1 $\mu\text{m}$ .

The first CXD experiments of this kind [3,5] have examined the internal structure of gold nanocrystals with volumes around 1 $\mu\text{m}^3$ . No optics, beside the monochromator, were introduced between the source and the sample, so the coherence is inherent to the source and monochromator. Conventional wisdom says that the introduction of optics, even Beryllium windows, can complicate the coherence, so should be avoided [6]. At the Advanced Photon Source (APS), these conditions gave sufficient intensity to measure CXD data with 30s exposures, usually divided between multiple accumulations of a few seconds to extend the dynamic range of the CCD. For this sample size, there is clearly enough intensity for the measurement. It is desired, however, to work with samples of 100nm size, which is just one order of magnitude smaller in linear dimension. Such a crystal has a volume of  $10^{-3}\mu\text{m}^3$  and would give a signal  $10^{-6}$  times weaker into the same detector, because of the corresponding broadening in reciprocal space. This would be very impractical to measure with current sources. Two orders of magnitude can be easily recovered by moving the detector ten times closer to the sample, exploiting the broader diffraction feature size. In principle, a third factor of ten can be recovered by using a monochromator with 10 times greater bandwidth, but this is hard to achieve in practice. So we are left with a signal  $10^4$  times weaker for the 100nm nanocrystals, which are of interest for their nanomaterial properties.

## 2. Experimental methods

For these reasons we are interested in introducing focussing optics to improve the flux on the sample. Louiville's theorem dictates that an increase of flux requires additional divergence of the beam. Fortunately we can sacrifice some excess lateral coherence, which is inversely proportional to divergence. The inherent coherence length of 5–100 $\mu\text{m}$  of the source can be reduced substantially while still illuminating a 100nm crystal coherently. In this paper, we explore this possibility in CXD experiments on 100nm "nanocubes" of silver by the introduction of Kirkpatrick-Baez (KB) mirror optics [7] in front of the sample.

We studied single crystalline silver nanocubes with a nominal size of 175nm [8]. The crystals were chemically synthesized by high temperature (160°C) reduction of silver nitrate in an ethylene glycol solvent with a polyvinyl pyrrolidone capping agent [8]. The nanocubes were dried from water suspension onto glass plates, then glued into place by drying methacrylate resin from a solvent. The gluing was found to be a generally inadequate precaution against radiation-induced movement of the samples. The nanocubes were occasionally found to be stable enough for a short series of measurements.

The CXD experiments were carried out at the ID-34-C beamline operated by UNICAT at the APS. Monochromatic X-rays with an energy of 8.5 keV were selected using a diamond (111) double crystal monochromator [9]. Each KB mirror of the pair employed a 4-cylinder bender with independent forces applied to each end [7]. The mirrors were uncoated trapezium-shaped silicon blanks polished to 1 Angstrom rms. The KB mirror system was mounted 52m from the source in a He environment with the horizontal-focussing mirror centered at 200mm in front of the sample and the vertical-focussing mirror at 100mm. The entrance aperture of the KB mirror system was set to 50(H) $\times$ 50(V)  $\mu\text{m}^2$  using vacuum roller-blade slits [10]. The focal spot size was determined by scanning a gold wire across the focus to be typically 1.5(H) $\times$ 1.0(V) $\mu\text{m}$  at the position of the sample. This is consistent with the expected demagnification of the source, considering that a secondary horizontal slit of 200 $\mu\text{m}$  was situated in the beamline at 25m. Diffraction data were recorded using a Roper Scientific direct-detection CCD with a pixel size of 22.5 $\mu\text{m}$  placed 1.2m behind the sample. Because it still provided sufficient oversampling, 4 $\times$ 4 grouping of the pixels was used in all the data included in this paper. The compound detector arm was set to the Bragg angle corresponding to the (111) reflection of silver. The sample orientation was adjusted until the diffraction from a single grain was centered on the CCD.

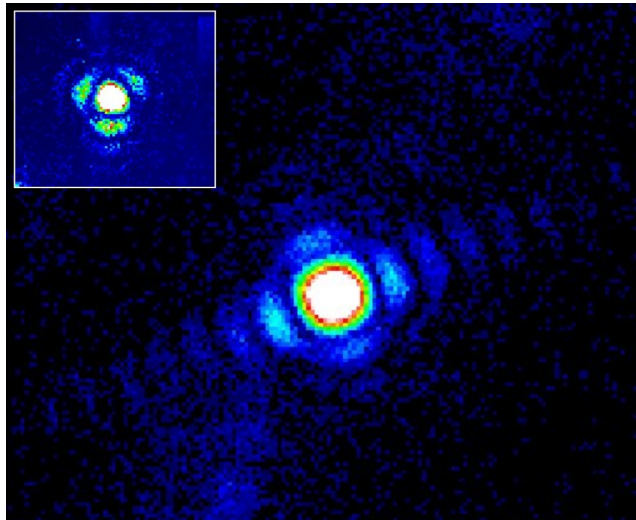


Fig. 1. Coherent X-ray Diffraction patterns recorded from a single silver nanocrystal. The full frame view is roughly centered on the rocking curve, while the inset is on the side.

### 3. Results of the experiment

Typical diffraction patterns are shown in Fig. 1. Certain views of the patterns, near the center of the rocking curve, were instantly recognisable as resembling a plus-shaped crossed-slit diffraction pattern. Other views were found to show approximate three-fold symmetry. The three-fold patterns were not centered on the rocking curve and were found to become inverted on the opposite side of the center, as expected for a centrosymmetric function in 3D. The patterns were qualitatively consistent with the cubic shapes of the crystals known from SEM [8]. The fringe spacing in Fig. 1 was 12 of the quadruple-sized pixels, corresponding to a cube-shaped sample with an edge of 162nm, slightly smaller than the value determined by SEM. The exposure time was 10s using a single accumulation of the CCD and the centers were found to be close to saturation. Compared with the  $1\mu\text{m}^3$  gold crystals, this represents an enormous enhancement of intensity.

We have made preliminary attempts at inverting the diffraction patterns using our iterative FFT method [3], so far without success. An important question, which we discuss here at some length is whether the distortions due to focussing the incident beam can spoil the coherence in such a way as to prevent inversion of the data. The simplest way that the diffraction pattern can be modified by the beam divergence is by *smearing*. If the focussed beam were composed of an incoherent superposition of plane waves coming at different source angles, multiple copies of the diffraction pattern would be added together on the detector and the sharp minima of the diffraction pattern of a simple slit would become significantly smeared. From the size of the entrance aperture, we calculate this smearing to be  $3(H)\times 7(V)$  of the quadruple pixels, which would cause significant loss of fringe visibility, especially in the vertical. This is not observed, at least to the extent just predicted. Clearly, the KB-focussed source must be considered to be a *coherent* convergent beam instead.

### 4. Discussion of curvature effects

Incident wave curvature effects can be predicted by straightforward ray tracing, as shown in Fig. 2. To a first approximation, the finite focus size can be attributed to demagnification of the source alone and hence ignored for a sample which is much smaller sized. It must be assumed nevertheless that the sample does not sit at the exact focus of the mirror but at a defocus distance,  $d$ , away.

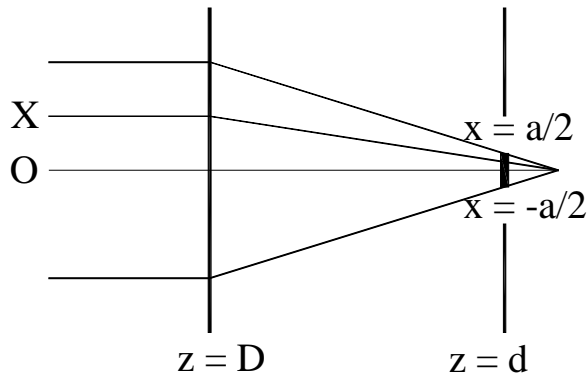


Fig. 2. Schematic ray tracing of the focusing geometry. The KB mirror is at a distance  $z=D$  if front of the focus, while the illuminated sample (thick vertical bar) is at  $z=d$ , the defocus distance. Ray O is the central ray, while ray X crosses the sample a distance  $x$  above the axis.

If the illuminating wave passing through the center of the sample is taken to have a phase of zero, then the phase shift at a lateral distance,  $x$ , away from the center can be found to be

$$\varphi(x) = k D (1 - \cos(x/d)) \approx \frac{1}{2} k D x^2 / d^2$$

where  $D$  is the focal length of the mirror and  $k$  is the X-ray wavevector. The curvature effects can be considered to be important when  $\varphi(x)$  reaches a significant fraction of  $\pi$  at the edges of the sample,  $x = a/2$ , where the sample size is  $a = 162\text{nm}$ . For the horizontal mirror ( $D=200\text{mm}$ ), this occurs at a defocus  $d=3.0\text{mm}$ , while for the vertical mirror ( $D=100\text{mm}$ ), this occurs at  $d=2.1\text{mm}$ . In spite of the careful focussing procedures used, it is conceivable that the mirrors were defocussed by this amount in our experiment because of the depth of field of the sample mount.

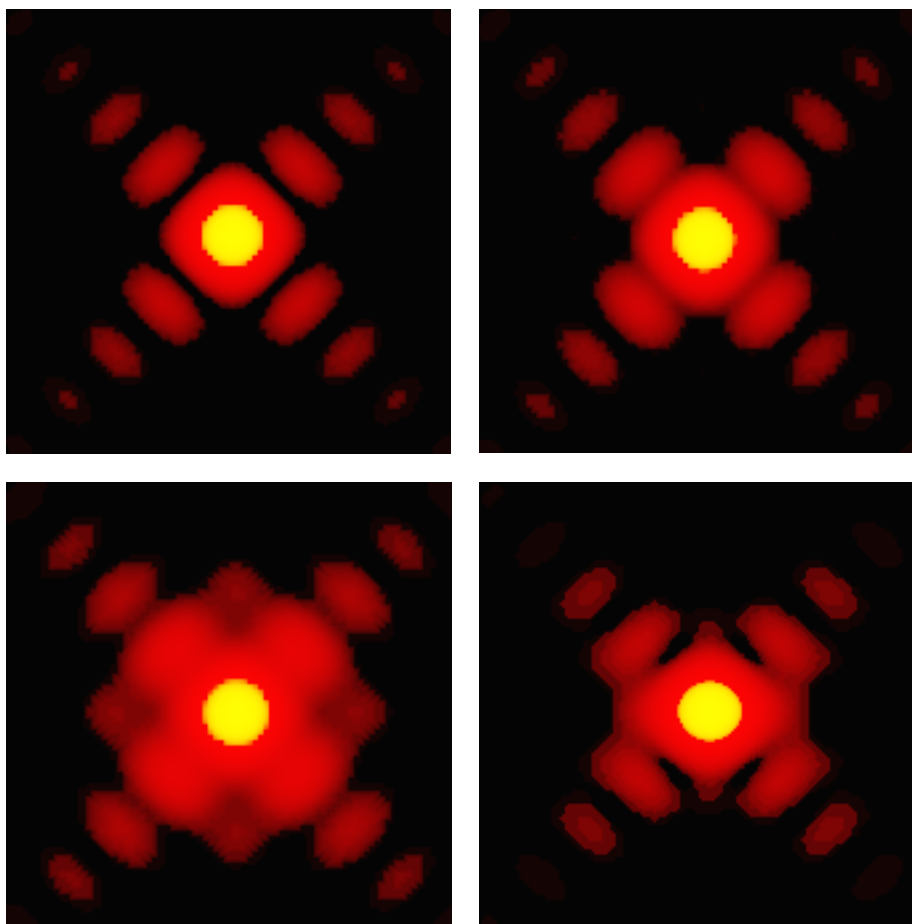


Fig. 3. Calculated far-field diffraction patterns for a cube, oriented diagonally, under different illumination conditions. Top left: plane wave. Top right: spherical wave with a phase shift of  $\pi/4$  at the cube edges. Bottom left: spherical wave with a phase shift of  $\pi/2$ . Bottom right: cylindrical wave with a phase shift of  $\pi/4$  in the horizontal only.

Figure 3 shows calculations of the diffraction patterns for an ideal cube-shaped sample, corresponding to the experimental conditions. Different amounts of wave curvature have been included, as indicated. The phase of the incident wave is assumed to vary quadratically across the sample. We note this is the smallest-order contribution that can affect the diffraction, since linear phase terms simply shift the position of the image. Even if the sample were significantly off axis in the experiment, this would only cause its diffraction pattern to appear shifted on the detector, but with the same amount of wavefront curvature. The magnitude of the curvature in Fig. 3 is specified by the total phase shift from the center to the edges of the sample.

Our calculations show that the introduction of this small amount of wavefront curvature is sufficient to change the diffraction patterns significantly, particularly the visibility of the inner fringes. We can estimate that, in the experimental data of Fig. 1, no strong curvature effects, beyond about  $\varphi(a/2) \sim \pi/4$ , have been seen so far. From one perspective, this is encouraging because it suggests that aberrations in the KB optics that introduce curvature must be unimportant [7]. Future experiments will attempt to look for the curvature effects which, as our calculations suggest, should be easy to detect. In particular, the case of a cylindrical incident wave field, where the foci of the two KB mirrors become separated by a millimeter or so, should lead to particularly dramatic effects on the diffraction patterns.

Once the curvature effects have been observed experimentally, it will open the possibility of new phasing methods based on the “Transport of Intensity” Equation (TIE) [11,12] that have the potential of resolving chiral structures and breaking the “twin” symmetry inherent in current iterative phasing methods. Specifically, the degrees of curvature would be separately varied in the horizontal and vertical directions by adjustment of the two independent KB mirrors. Two through-focal series would be used in a difference calculation that would result directly in a measured phase [13]. It is believed that just three diffraction patterns would be sufficient to determine the phase uniquely [13].

## 5. Conclusions

The following general conclusions could be drawn from the experimental results: Firstly and most importantly, the high-resolution diffraction patterns clearly demonstrate the feasibility of carrying out such measurements on single nanocrystals with a size in the nanometer range. Depending on the orientation of the individual nanocrystals the measured diffraction patterns showed nice three- and four-fold symmetry and typically 5 to 10 high contrast interference fringes in directions corresponding to the facets of the cubic shape of the crystals. Furthermore, we have investigated, but did not find, any negative effects on the transverse coherence arising from using the crucially important KB focusing optics to increase the intensity. Finally, the results obtained agree qualitatively with model calculations based on a simple Fourier transform of a two-dimensionally projected single silver nanocube. Encouraged by this successful first demonstration experiment of coherent x-ray diffraction on sub-micrometer single crystalline nano-objects we plan to work on the direct reconstruction of a full 3D diffraction data by using the oversampling phasing method as used previously [3] or by the TIE from a through-focal series of diffraction patterns [11-13].

## 6. Note added in proof

Since the original submission of this manuscript, the inversion of diffraction patterns similar to Fig. 1 has been successful and will be published in a future communication. This result adds weight to the arguments made here that the diffraction patterns contain few distortions attributable to the introduction of optics.

## Acknowledgements

This work was supported by the NSF under grant DMR 03-08660. The 34-ID-C Coherent X-ray Diffraction facility was built with funds from NSF DMR 97-24294. The UNICAT facility is supported by the University of Illinois Materials Research Laboratory, funded by U.S. Department of Energy (DOE) under DEFG02-91ER45439, Oak Ridge National Laboratory, the National Institute of Standards and Technologies, and UOP Research & Development. The APS is itself supported by the DOE under contract No. W-31-109-ENG-38.